

Wigner crystals of ions as quantum hard drives

J. M. Taylor¹ and T. Calarco^{2,3}

¹*Department of Physics, Massachusetts Institute of Technology, Cambridge, Massachusetts 02139, USA*

²*Department of Physics, Harvard University, and Institute for Theoretical Atomic, Molecular, and Optical Physics, Cambridge, Massachusetts 02138, USA*

³*Institute of Quantum Information Processing, Ulm University, D-89081 Ulm, Germany*

(Received 13 June 2007; revised manuscript received 19 November 2007; published 18 December 2008)

Atomic systems in regular lattices are intriguing systems for implementing ideas in quantum simulation and information processing. Focusing on laser-cooled ions forming Wigner crystals in Penning traps, we find a robust and simple approach to engineering nontrivial two-body interactions sufficient for universal quantum computation. We then consider extensions of our approach to the fast generation of large cluster states and a nonlocal architecture using an asymmetric entanglement generation procedure between a Penning trap system and well-established linear Paul trap designs.

DOI: [10.1103/PhysRevA.78.062331](https://doi.org/10.1103/PhysRevA.78.062331)

PACS number(s): 03.67.Lx, 37.20.+j, 37.10.De

I. INTRODUCTION

Quantum information processing using trapped ions has been the focus of theoretical [1] and experimental [2–6] efforts over the past decade. The coherence times of ions can exceed seconds, while manipulation and entanglement time scales can be as fast as tens of microseconds. So far, approaches to scaling these systems to many ions have met with significant issues, both in linear Paul trap systems, where increasing numbers of ions leads to control difficulties, and in proposed more complex trap arrays, where “shuttling” of quantum information using gate electrodes would allow for a scalable architecture [7]. A system-level solution is to separate the processing elements (processor qubits) from the memory [8].

One natural system to consider as a quantum memory is a Wigner crystal of ions in a Penning trap [9]. Such crystals can be robustly formed [10] and are dynamically stable, with tens of thousands of ions in a given trap. In addition, the strength of the Coulomb interaction leads to large separations between individual ions, making individual addressing of ions in such lattices a distinct possibility, in contrast to present control in neutral atom and polar molecule lattices [11,12].

In this article we develop an approach to quantum memory and entanglement generation that takes full advantage of the advances in ion trap technology for building large Wigner crystals of ions in Penning traps. Such higher-dimensional crystals have advantages, both in ion number and in construction simplicity, when compared to multizone Paul traps, at the cost of substantial difficulties with many phonon modes. However, by using a modulated-carrier “push” gate that is a variation on existing linear ion trap quantum computing schemes [13–16], we find a fast but adiabatic method for building small clusters of entanglement which is insensitive to thermal phonons in two-dimensional (2D) and 3D Wigner crystals. We take advantage of some of the unique features of Penning traps, such as rotation of the crystal, to provide simplifications in the necessary hardware to implement these ideas in 2D Wigner crystals. A 3D generalization of our scheme could as well be applied to ion

crystals in Paul traps. We further show that such a quantum memory device can also be used directly for cluster-state quantum computation. Our approach follows recent work [17] on performing quantum gates in 2D Wigner crystals. Finally, nondeterministic entanglement generation between distant ions suggests a processor (linear Paul trap) and memory (2D Wigner crystal) architecture based upon a quantum register approach [8,18], where the low photon collection efficiency from ions in the memory is offset by an asymmetric entanglement generation scheme using a weak cavity coupled to ions in the processor [3,19,20].

We start by considering a Wigner crystal of ions, rotating in a Penning trap [9] with harmonic confinement with frequencies ω_{xy} (in the lateral directions) and ω_z (in the vertical direction). With characteristic ion spacings $d \sim 10 \mu\text{m}$, tightly focused lasers allow for individual addressing of ions (see Fig. 1). Laser cooling can reduce the temperature $\approx 1 \text{ mK}$, yielding on the order of $10^2 - 10^3$ phonons in the softest (lateral) modes. By using long-lived, metastable states of the ions as a quantum memory, we may neglect memory errors in our discussion. A tightly focused laser allows for nearest-neighbor phase gates and for single-ion operations. Large-scale computation may be considered using either nearest-neighbor couplings or via a variety of quantum communication techniques developed for quantum repeater pro-

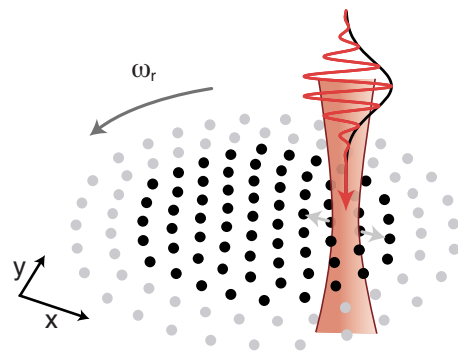


FIG. 1. (Color online) Two-qubit gate via intensity modulation of a laser addressing a pair of ions in a crystal rotating at frequency ω_r .

TOCOLS. When used in conjunction with the deterministic phase gate developed below and local single-ion operations (implemented, e.g., via Raman transitions), this will suffice for performing large-scale quantum algorithms [18] by using the remote controlled-NOT (CNOT) gate [21].

II. MODULATED-CARRIER GATE

A spatially inhomogeneous laser detuned from the appropriate transitions between internal (qubit) states of an ion (a two-level system with Pauli matrices $\sigma_i^{x,y,z}$) produces a ponderomotive force \vec{f}_i due to the gradient in its intensity. Using an appropriate combination of polarizations and frequencies, in analogy with alkali-metal atoms [22], the sign of the force becomes dependent upon the internal state of the ion, with the associated perturbation to the system:

$$V = \sum_i [\vec{x}_i \cdot \vec{f}_i(t)] \sigma_i^z, \quad (1)$$

where \vec{x}_i is the displacement of ion i away from its equilibrium position. The latter can take place either along the separation between two individual ion microtraps [14] or perpendicularly to the plane of an ion Wigner crystal in a Penning trap [17]. In both schemes, as the ion displacements are coupled (via phonons), such a push leads to an effective $\sigma_i^z \sigma_j^z$ interaction. Adiabaticity is required for vibrational excitations to be absent after the gate. This bounds the clock speed to be lower than the frequency of trapping in the push direction: tight traps are needed for fast, temperature-insensitive operation.

Carrier push derivation

We now introduce a simple variant of the fast-kick “push” gate which allows us to use even the soft (lateral) modes when their temperature is extremely high. Our variant uses slow modulation of a fast, oscillating state-dependent force, and thus it can be regarded as a hybrid between fast-kick “bang-bang” decoherence control and continuous pulse shaping schemes. The oscillation averages any ion motion to zero over the course of the gate, while the in-phase oscillation of nearby ions leads to a nontrivial phase evolution and the desired quantum gate between ions in the crystal. In addition, as our gate allows for nontrivial oscillation of ion positions in all three spatial dimensions (versus only in the tightly confined direction for the vertical push gate), it can work using a single laser beam and in three-dimensional crystals.

It is instructive to recall the general description of “push” phase gates when in a complex crystal [15,17]. We start by rewriting the Hamiltonian of N interacting ions to second order in displacement from the equilibrium positions, $H = \sum_K \hbar \omega_K \hat{a}_K^\dagger \hat{a}_K$, using normal-mode coordinates indexed by $K = \{\vec{k}, \lambda\}$ (the wave vector and polarization), $\vec{x}_i = \sum_K M_{iK} \vec{e}_K (\alpha_K / \sqrt{2}) (\hat{a}_K + \hat{a}_K^\dagger)$. The $\alpha_K = \sqrt{\hbar / m \omega_K}$ are the oscillator ground-state lengths; the matrix M is orthogonal ($M^T M = M M^T = 1$). The perturbation V can now be written as

$$V = \sum_K \alpha_K f_K(t) (\hat{a}_K^\dagger + \hat{a}_K) / \sqrt{2}, \quad (2)$$

where $f_K(t) = \sum_i M_{iK} [\vec{e}_K \cdot \vec{f}_i(t)]$ is the state-dependent force on normal mode K defined via the transformation M and Eq. (1).

The problem factorizes into $3N$ independent, driven oscillators. For scenarios with $\lim_{t \rightarrow \pm \infty} f(t) = 0$, the oscillator evolution is given by the unitary transform $U_K(t) = e^{-i\phi_K(t)} \exp(\beta_K \hat{a}_K^\dagger - \beta_K^* \hat{a}_K)$, where ϕ_K and β_K satisfy the differential equations [15]

$$\dot{\beta}_K = -i\omega_K \beta_K + i \frac{\alpha_K}{\hbar \sqrt{2}} f_K(t), \quad \dot{\phi}_K = \frac{\alpha_K}{\hbar \sqrt{2}} f_K(t) \text{Re}[\beta_K(t)] \quad (3)$$

which are exact to second order.

We now seek an approach which still maintains no net change in displacement and no dependence of the overall phase on phonon state, but can operate on faster time scales—on the order of ω_K . To this end, we add a sinusoidal variation to the force [$f(t) \rightarrow \cos(\nu t) f(t)$], with $\nu \gg \omega_K$ for modes K that are coupled to the force. For example, a lateral push (used in what follows) only couples to the lateral phonon modes near the frequency ω_{xy} and is insensitive to the vertical phonon modes near frequency ω_z . Qualitatively, this averages out any net displacement: while many more ions are excited during the process than just the two involved in gate operation, at the end no entanglement remains between the latter and the surrounding crystal. We also checked that such a carrier modulation makes single-qubit phases vanish. The force sign change can be obtained by a single laser beam with time-varying polarization, thereby avoiding dissipation by low-detuning-enhanced spontaneous emission and single-qubit phase errors due to amplitude fluctuations. If τ denotes the time scale associated with the modulation $f(t)$, assuming $\nu \gg \tau^{-1}$, we can perform adiabatic elimination and get a gate with the same desirable properties that can also operate nontrivially on arbitrarily “soft” phonon modes at very high temperatures. To this aim, we choose the ansatz $\beta = \beta_+ e^{i\nu t} + \beta_- e^{-i\nu t}$ (subscripts omitted for clarity). Adiabatic elimination by setting $\dot{\beta} = 0$ yields $\beta_{\pm} = \alpha f(t) / [2\sqrt{2}\hbar(\omega \pm \nu)]$. We find that the displacement of a normal mode induced by the gate is proportional to the force applied and can be made zero independent of the initial phonon state by starting and ending with zero force. This eliminates any potential error due to entanglement between phonons and the internal states of the ions.

In this approach, the differential equation for phase now reads

$$\dot{\phi} = \frac{\alpha^2}{2\hbar^2} f^2(t) \frac{\omega}{(\omega^2 - \nu^2)} \cos^2(\nu t). \quad (4)$$

Averaging the quickly varying component lets us replace $\cos^2(\nu t)$ with $1/2$. Returning the mode index K , we find that the overall phase accumulated, $\sum_K \phi_K(\tau)$, for a gate occurring over a time 0 to τ does not depend on the phonon initial state. However, the internal states of the ions are affected by

the unitary $\exp(-i\sum_{ij}\phi_{ij}\sigma_i^z\sigma_j^z)$ where the two-body phases are given by

$$\phi_{ij} = \sum_{\lambda} S_{ij}^{\lambda} \int_0^{\tau} [\vec{f}_i(t) \cdot \vec{e}_{\lambda}] [\vec{f}_j(t) \cdot \vec{e}_{\lambda}] dt. \quad (5)$$

The pulse-shape-independent form factor is

$$S_{ij}^{\lambda} = - \sum_k \frac{\alpha_{k,\lambda}^2 \omega_{k,\lambda}}{4\hbar^2(\nu^2 - \omega_{k,\lambda}^2)} M_{ik,\lambda} M_{jk,\lambda} \quad (6)$$

(the polarization vectors \vec{e}_K only depend on λ).

Expanding in inverse powers of the large carrier frequency ν , we note that the first term $O(\nu^{-2})$ is proportional to $\sum_k M_{ik,\lambda} M_{jk,\lambda} = 0$ (due to the orthogonality of the matrix M). The first nonzero term is $O(\nu^{-4})$. This is similar to the result for adiabatic gates, where the averaging of motion occurs from an intrinsic trapping frequency ω . Compared to adiabatic gates (operating over a time scale much longer than $1/\omega$), this modulated-carrier push gate is inverted in sign and differing in phase by a factor $(\omega/\nu)^4/2$. For example, in comparison to the vertical push gate, with $\omega = \omega_z$, the modulated carrier gate operating with lateral motion and with $\omega_z \gg \nu \gg \omega_{xy}$ has much more phase accumulated for the same laser parameters. On the other hand, in comparison to a lateral push gate, with $\omega = \omega_{xy}$, the modulated carrier gate accumulates much less phase for the same laser parameters.

III. PERFORMANCE

To investigate the performance of our proposed gate with a mesoscopic crystal, we performed numerical simulations of the modulated-carrier gate for 2D and 3D Wigner crystals ($N=147$ shown in Fig. 2). We started by doing a Monte Carlo minimization of the momentum-independent components of the Hamiltonian in the rotating frame:

$$V_{\text{tot}} = \sum_i \frac{m}{2} (\omega_z^2 z_i^2 + \omega_{xy}^2 r_i^2) + \frac{1}{2} \sum_{i \neq j} \frac{e^2}{4\pi\epsilon_0 |r_i - r_j|}. \quad (7)$$

We remark that this minimization is equivalent to finding the Gibbs distribution for the mesoscopic system at zero temperature [9]. The 2D crystal is shown in Fig. 1 in isometric projection. Expanding to second order in displacements from this configuration, the normal-mode coordinates were found; the phonon modes calculated from this configuration are shown in Figs. 2(a) and 2(b).

To compare to the equivalent adiabatic gate (using lateral pushes) and the proposed vertical push gate of Ref. [17], we considered the purity of the final, entangled state as a function of temperature (Fig. 2). To do so, we calculated the final displacement of mode K , $\beta_K^{\text{even(odd)}}$, exactly using Eq. (3) for even (odd) parity spin states of the qubits, as the gate operation is the same for two qubit states of the same parity. We determined the necessary lateral forces on qubits i and j , $f_i = f_j = P\hbar\omega_{xy} \cos(\nu t) \exp[-(t/\tau)^2] / |r_i - r_j|$, to produce a π phase between the two chosen qubits where P is a dimensionless parameter set to achieve a π phase. We then calculated the overlap of the final state on the desired (entangled) state, tracing out of the phonon modes. This fidelity was

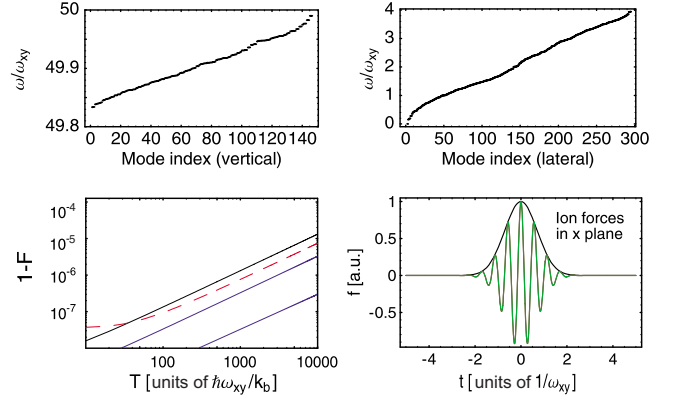


FIG. 2. (Color online) Phonon spectrum (top) for vertical and lateral phonons for a trap with $N=147$ ions and $\omega_z/\omega_{xy}=50$. Bottom left: Fidelity versus temperature for the vertical push gate of Ref. [17] (red-dashed line) and for the modulated carrier gate with $\nu = 11\omega_{xy}$ between different ion pairs: at the center (upper solid line), as well as two (middle solid line) and four (lower solid line) lattice sites away from the center. Bottom right: Modulated carrier gate's and vertical push gate's forces on one of the two ions over the gate time; both gates operate in a time $\tau \sim 1/\omega_{xy}$. Anharmonic corrections to the fidelity are not included here. For this choice of parameters, the vertical push gate [17] requires 20 times the force (and laser power) of our modulated carrier gate to achieve the same final π two-body phase.

minimized over initial qubit states and gives the final, minimum fidelity

$$F = \text{Min}_{g=\text{even,odd}} \prod_K \exp \left[-P^2 \frac{|\beta_K^g|^2/4}{1 - e^{-\omega_K/k_B T}} \right]. \quad (8)$$

In these calculations the vector potential in the crystalline (rotating) frame was neglected; its inclusion does not qualitatively change our results. We calculated the fidelity as a function of temperature for adjacent pairs of ions at the center of the crystal and two and four lattice sites from the center. The infidelity ($1-F$) is shown in Fig. 2.

Fixing the time τ for performing a gate, we find that the ratio of forces (i.e., laser power) required for achieving a π phase for the vertical push gate and for the modulated carrier gate goes as $(\omega_z/\nu)^2$. This is due to the ω_z^2 dependence of the force for the vertical push gate, while our scheme has a ν^2 dependence. In essence, the lower frequency of the carrier allows for larger displacements for the same laser power, increasing the phase evolution. Thus, the modulated carrier gate requires substantially less laser power for the same conditions with negligible reduction in fidelity. Alternatively, fixing laser power, the gate time could be reduced, enhancing the overall performance of quantum information protocols. For specificity, setting $\omega_{xy}=200$ kHz, $\omega_z=10$ MHz, and a gate time $\tau=5$ μ s, we find that $\nu=2.2$ MHz provides $1-F < 10^{-5}$ with negligible heating. Even smaller errors are found in simulations of the 3D crystal under the same approximations.

A practical limitation occurs due to the spontaneous emission induced by the off-resonant laser interactions. Tight focusing increases the force for the same laser power; thus,

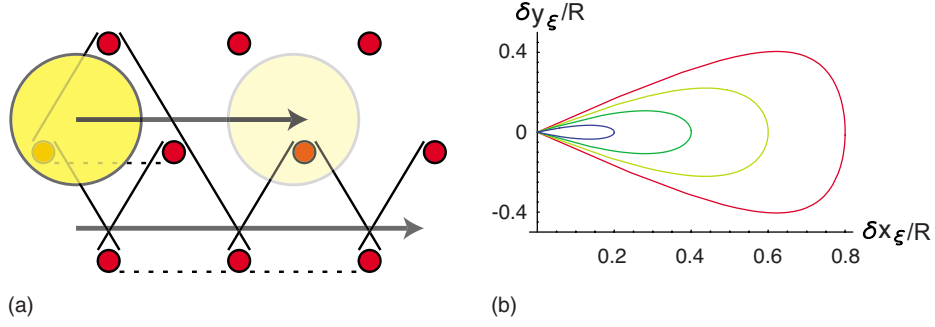


FIG. 3. (Color online) (a) A laser is swept adiabatically from left to right, leading to a weighted graph state with different phases for solid and dashed lines. (b) Laser displacements in the crystal plane needed to obtain a constant sweep velocity at given distances $\xi/R = 0.2, 0.4, 0.6, 0.8$ (from innermost to outermost) from the center, in the rotating crystal's frame.

using a pair of adjacent, narrow-waist ($\leq 2 \mu\text{m}$) laser beams reduces spontaneous emission and power requirements. For specificity, using a transition with spontaneous emission of $\gamma = 20$ MHz and lasers with peak Rabi frequency of 100 GHz detuned 100 THz from the atomic transition, a laser power of ~ 3 mW per beam is required for our gate, with an induced error of $\leq 0.1\%$ per gate.

IV. QUANTUM CLUSTER-STATE GENERATION

We now consider an approach that takes advantage of the Coulomb interactions in the lattice to create and dynamically extend a cluster state for universal measurement-based computation. Specifically, the goal is to obtain a weighted-graph state $\exp(i\sum_{ij}\sigma_i^z\sigma_j^z\vartheta_{ij}/2)|+\dots+\rangle$, where in the ideal case ϑ_{ij} equals π between nearest neighbors on a square lattice and zero otherwise. On a triangular lattice like the one available in many-ion Penning traps, this can be achieved if ϑ_{ij} is made to vanish along one side of each lattice cell and to be π on the other two. The idea is to obtain this via a global $\pi/2$ qubit rotation followed by a push gate acting on all three cell vertices at the same time, possibly with a laser swept at constant velocity through the cell itself, to take advantage of the uniform circular motion of the lattice.

We start by considering a focused laser beam, modulated at a frequency $\nu \gg \omega_{xy}$ and of waist σ (in units of the lattice length d), swept at constant velocity v through the Wigner crystal, along a direction parallel to one of the lattice vectors (Fig. 3), at half the height of a triangular cell. The sweep rate is set such that $d/v \sim \tau = 5 \mu\text{s}$ —i.e., that as the laser goes by it induces a modulated carrier gate between nearby ions. The effect of this sweep is, apart from a global single-qubit rotation, to generate a weighted-graph phase, where ϑ_{ij} takes value $\varepsilon\theta(\omega)$ on the cell side that is parallel to the sweep direction and $\theta(\omega)$ on the other two sides, with $\varepsilon = e^{-3/(8\sigma^2)}(11 - 8\sigma^2)/(\sigma^2 + 8)$, while

$$\theta(\omega) = \frac{\Omega_0^4}{\omega^2 \Delta^2} \frac{\alpha^4}{d^4} \frac{q^2}{\hbar \epsilon_0 v} \frac{e^{-1/(2\sigma^2)}}{\sqrt{8\pi\sigma}} \left(\frac{1}{\sigma^2} + \frac{1}{8} \right), \quad (9)$$

where $\alpha = \sqrt{\hbar/(m\omega)}$, Ω_0 is the peak Rabi frequency corresponding to the center of the laser beam, Δ is its detuning from the ion's internal transition, and q is the electron charge. Using the fast carrier modulation described above,

the semiclassical calculation of Eq. (9) is no longer valid, but the discussion of Eq. (6) shows that the resulting phase is simply $-\theta(\nu)/2$. A cluster state is then obtained by making ε small via an appropriate choice of the laser waist (numerically, $\sigma \leq 0.2$), while tuning $\theta(\nu)/2$ to π by adjusting the other experimental parameters such as laser power. A detailed analysis in this sense, as well as concerning errors from imperfect fulfilling of the adiabaticity condition, has been presented in [23]. The primary error for sweep rates $v = d/5 \mu\text{s}$ (where the infidelity from finite temperature and nonadiabatic effects, shown in Fig. 2, is less than 0.01%) is given by the residual phase on the dashed lines of Fig. 3. The resulting cluster-state fidelity per qubit can be calculated by considering the expectation value of the stabilizer of the cluster-state at site i : $S_i = Z_i \prod \langle ij \rangle X_j$. We find $\langle S_i \rangle = |\frac{1 + \cos(2\varepsilon\pi)}{2}|^2 \approx 1 - 2\pi^2\varepsilon^2$.

Care needs to be taken to ensure a sweep having a given distance ξ from the trap center and velocity v in the rotating crystal's frame. To this end we apply to the laser, initially focused at a distance R from the center, a displacement $\delta \mathbf{d}_\xi(t) = \{\delta x_\xi(t), \delta y_\xi(t)\}$ of the form

$$\delta x_\xi(t) = [R - \xi/\cos(\omega_r t)]\Theta(\chi - |\omega_r t|), \quad (10)$$

$$\delta y_\xi(t) = \xi[\omega_r t \tan(\chi)/\chi - \tan(\omega_r t)]\Theta(\chi - |\omega_r t|) \quad (11)$$

(see Fig. 3), where $\chi \equiv \arccos(\xi/R)$. Cluster-state generation as presented uses a single laser beam, resulting in substantially higher-laser-power requirements than the two-qubit gate with two beams as described above. In particular, to achieve an error $2\pi^2\varepsilon^2 \leq 0.1\%$, a detuning of 200 THz and peak Rabi frequency of 4 THz (corresponding to 5 W of laser power) would be required.

V. ASYMMETRIC ENTANGLEMENT GENERATION

We conclude with a brief discussion on the implementation of circuit-based computation. In principle, the modulated carrier gate allows for long-distance operations. However, only low-frequency phonon modes are excited, requiring long gate times and leading to higher errors for fixed temperature. Thus an alternative approach may be necessary. We consider using entanglement generation like first proposed in [24,25] and remote CNOT gates to overcome this

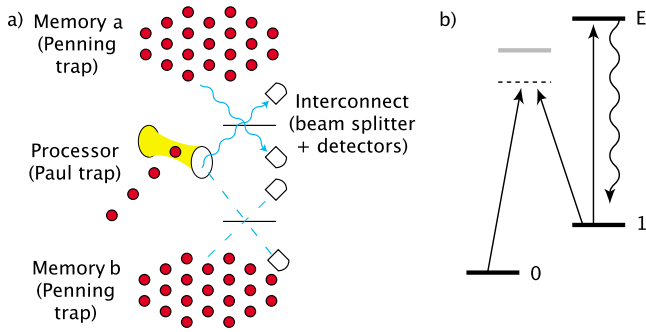


FIG. 4. (Color online) (a) Schematic of a quantum processor (such as a linear Paul trap) coupled via a high-finesse cavity to a photodetector system to allow interference with photons from an ion Wigner crystal in Penning trap(s) nearby. Gates between distant ions within the memory are achieved by sequential entanglement between each ion and an ion in the quantum processor, followed by entanglement swapping via Bell measurement of the ions in the quantum processor and teleportation-based gates. (b) Ion-level structure for state-dependent fluorescence (cycling between E and 1) and for single-qubit operations via Raman coupling (1 to 0 rotations with off-resonant beams through the gray intermediate state).

problem. While we could directly generate entanglement between two ions in the same (or different) Penning traps via state-dependent fluorescence, we anticipate that low photon collection efficiency will limit the utility of the direct approach.

Instead, we use a quantum processor unit (such as a linear Paul trap) separated from the quantum memory unit (our Wigner-crystal-based quantum hard drive—see Fig. 4), characterized by photon collection efficiencies η' and η , respectively. Without loss of generality, we will assume $\eta' > \eta$, as can be achieved via coupling with high-finesse cavities [3,19]. For this asymmetric scenario, we use a “double-heralded” approach, first introduced in Ref. [20]. Indeed, the asymmetry between memory and processor present in our scenario requires a symmetrization procedure involving two subsequent photon detections, or “clicks,” as opposed to existing “single-click” entanglement generation schemes [26]. On the other hand, here we take advantage of the higher-efficiency processor-side photodetection to enhance the overall entanglement-generation rate. Our two-click asymmetric entanglement-generation procedure starts with an equally weighted superposition $|+\rangle = |0\rangle + |1\rangle$. An optical π pulse leads to spontaneous emission of a single photon at a rate γ from the $|1\rangle \leftrightarrow |E\rangle$ transition. Then the photons are interfered

with on a beam splitter. Without assuming photon-number-resolving detectors, the state after one click becomes

$$\eta' |\psi_{\pm}\rangle \langle \psi_{\pm}| + O(\eta') |11\rangle \langle 11|, \quad (12)$$

with $|\psi_{\pm}\rangle \equiv (\sqrt{\eta/\eta'} |01\rangle \pm |10\rangle)$. To symmetrize the entangled state and simultaneously remove the $|11\rangle$ component, a π pulse between the metastable states ($|1\rangle \leftrightarrow |0\rangle$) followed by repetition of the above protocol results in a pure state $|\Phi^+\rangle = (|01\rangle \pm |10\rangle)/\sqrt{2}$. The overall procedure succeeds with probability $\eta\eta'$, indicating that the time required is $(\gamma\eta\eta')^{-1}$. A standard one-click scheme with excitation probability p [26]—i.e., starting from a state $\sqrt{1-p}|0\rangle + \sqrt{p}|1\rangle$ (where $p \ll 1$ determines the final infidelity of the entangled state) rather than $|+\rangle$ as above—takes a time $(\gamma\eta p)^{-1}$ and succeeds with probability ηp , which is generally $\ll \eta\eta'$, assuming that the processor-side photodetection efficiency η' exceeds the infidelity p one is willing to tolerate. In other words, the higher fidelity a pair one wishes to generate, the longer it takes. By contrast, in our scheme the fidelity can be high without a further increase in generation time, because we take advantage of the efficient coupling between the processor ion and the cavity.

Thus, for large-scale computation, a central processor unit with high collection efficiency allows for high-fidelity gates between elements of the “hard drive” memory on a time scale $2/\gamma\eta\eta'$ (see Ref. [18] for further improvements). For concreteness, we take a radiative decay rate of $\gamma = (2\pi) \times 10$ MHz, $\eta = 10^{-3}$ (confocal approach with low-numerical-aperture lens), and desired infidelity $1 - F < 10^{-4}$. Entanglement generation between two such ions would take a time ~ 10 ms or longer; in contrast, for $\eta' \sim 0.1$, using the intermediate quantum processor leads to entanglement generation between processor and both ions in a time of order $100 \mu\text{s}$, comparable to the phase gate operation times already discussed.

This complements the quantum hard drive architecture described above, providing a comprehensive toolbox for universal quantum computation with ion crystals in Penning traps that relies on existing technologies under available experimental conditions.

ACKNOWLEDGMENTS

We thank J. Bollinger, D. Porras, P. Zoller, R. Blatt, and A. Micheli for helpful discussions. J.M.T. is supported by Pappalardo and T.C. by the European Commission through projects SCALA and QOQIP.

[1] J. I. Cirac and P. Zoller, *Phys. Today* **57** (3), 38 (2004).
 [2] F. Schmidt-Kaler *et al.*, *Nature (London)* **422**, 408 (2003).
 [3] B. B. Blinov *et al.*, *Nature (London)* **428**, 153 (2004).
 [4] J. Chiaverini *et al.*, *Science* **308**, 997 (2005).
 [5] C. Langer *et al.*, *Phys. Rev. Lett.* **95**, 060502 (2005).
 [6] M. M. Boyd *et al.*, *Science* **314**, 1430 (2006).
 [7] D. Kielpinski, C. Monroe, and D. Wineland, *Nature (London)*

417, 709 (2002).
 [8] M. Oskin, F. T. Chong, and I. L. Chuang, *IEEE Trans. Comput.* **18**, 79 (2002).
 [9] D. H. E. Dubin and T. M. O’Neil, *Rev. Mod. Phys.* **71**, 87 (1999).
 [10] M. J. Jensen, T. Hasegawa, and J. J. Bollinger, *Phys. Rev. A* **70**, 033401 (2004).

- [11] I. Bloch, *Nat. Phys.* **1**, 23 (2005).
- [12] H. P. Büchler, E. Demler, M. Lukin, A. Micheli, N. Prokof'ev, G. Pupillo, and P. Zoller, *Phys. Rev. Lett.* **98**, 060404 (2007).
- [13] A. Sørensen and K. Mølmer, *Phys. Rev. Lett.* **82**, 1971 (1999).
- [14] J. I. Cirac and P. Zoller, *Nature (London)* **404**, 579 (2000); T. Calarco, J. I. Cirac, and P. Zoller, *Phys. Rev. A* **63**, 062304 (2001).
- [15] J. J. García-Ripoll, P. Zoller, and J. I. Cirac, *Phys. Rev. Lett.* **91**, 157901 (2003); *Phys. Rev. A* **71**, 062309 (2005).
- [16] S.-L. Zhu, C. Monroe, and L.-M. Duan, *Europhys. Lett.* **73**, 485 (2006).
- [17] D. Porras and J. I. Cirac, *Phys. Rev. Lett.* **96**, 250501 (2006).
- [18] L. Jiang, J. M. Taylor, A. S. Sorensen, and M. D. Lukin, e-print [arXiv:quant-ph/0703029](https://arxiv.org/abs/quant-ph/0703029); L. Jiang, J. M. Taylor, A. S. Sorensen, and M. D. Lukin, *Phys. Rev. A* **76**, 062323 (2007).
- [19] A. B. Mundt, A. Kreuter, C. Becher, D. Leibfried, J. Eschner, F. Schmidt-Kaler, and R. Blatt, *Phys. Rev. Lett.* **89**, 103001 (2002).
- [20] S. D. Barrett and P. Kok, *Phys. Rev. A* **71**, 060310(R) (2005).
- [21] D. Gottesman and I. L. Chuang, *Nature (London)* **402**, 390 (1999).
- [22] D. Jaksch, H. J. Briegel, J. I. Cirac, C. W. Gardiner, and P. Zoller, *Phys. Rev. Lett.* **82**, 1975 (1999).
- [23] M. Sasura and A. M. Steane, *Phys. Rev. A* **67**, 062318 (2003).
- [24] C. Cabrillo, J. I. Cirac, P. Garcia-Fernandez, and P. Zoller, *Phys. Rev. A* **59**, 1025 (1999).
- [25] S. Bose, P. L. Knight, M. B. Plenio, and V. Vedral, *Phys. Rev. Lett.* **83**, 5158 (1999).
- [26] L. Childress, J. M. Taylor, A. S. Sorensen, and M. D. Lukin, *Phys. Rev. A* **72**, 052330 (2005).